Supplementary Material to the article

"Slow oscillations of transverse magnetoresistance in $HoTe_3$"

Supplementary Note 1

Tight Binding model of RTe_3

The electronic band structure in the quasi-two-dimensional RTe_3 can be well approximated by the elementary tight binding (TB) model of the in-plane Te $5p_{x/y}$ orbitals, which yields the following dispersions:

$$\epsilon_{px}(k_x,k_y)=-2t_{para}\cos[k_x a_0]-2t_{perp}\cos[k_y a_0]-E_F$$
$$\epsilon_{py}(k_x,k_y)=-2t_{para}\cos[k_y a_0]-2t_{perp}\cos[k_x a_0]-E_F \quad (1)$$

where $a_0 \approx c_0$ is the 2D in-plane lattice constant with magnitude $\sqrt{2}$ smaller than that of the 3D unit cell. The Fermi energy E_F is determined from the electron density, namely from the condition of 1.25 electrons for each p_x and p_y orbitals [1]

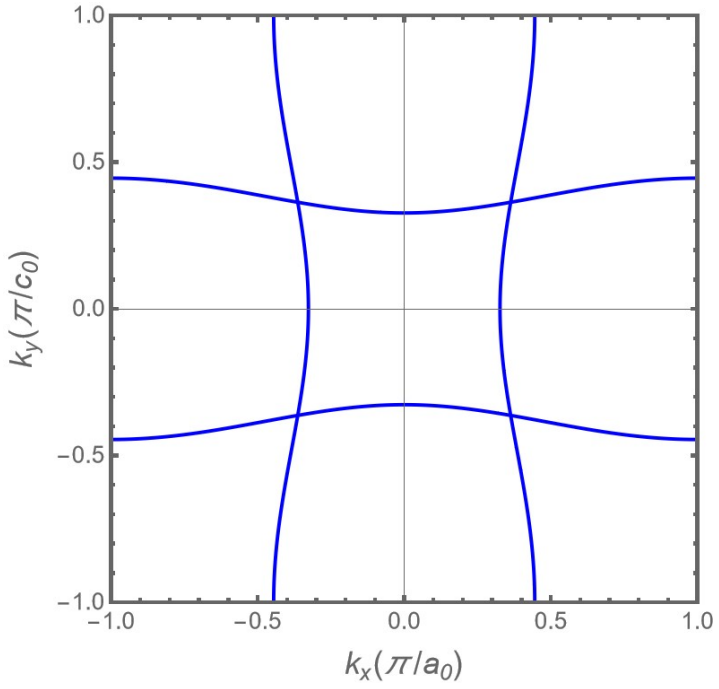

Fig. S1. 2D Fermi Surface (FS) of $HoTe_3$ calculated by TB model, using $t_{para} = -1.96$ eV and $t_{perp} = 0.34$ eV and $E_F = -1.35$ eV [1].

The main (bare) bands of the non-interacting TB model, shown in Fig. S1, gain a small curvature proportional to the ratio t_{perp}/t_{para} leading to the diamond-shaped Fermi surface. The CDW transition takes place when there is a permanent lattice distortion at some wave vector $\mathbf{Q}_{CDW}$. Taking the mean-field approach, the lattice distortion leads to a coupling between the states $|k\rangle$ and $|k \pm Q_{CDW}\rangle$ with an interaction strength of Δ. Hence, the new electronic eigenstates $|\psi_k\rangle$ can be written as a superposition of the original states

$$|\psi_k\rangle = u_{k-Q_{CDW}} ¿$$

and are the eigenstates of the following matrix [2]:

$$\begin{bmatrix} \epsilon_{k-Q_{CDW}} & \Delta & 0 \\ \Delta & \epsilon_k & \Delta \\ 0 & \Delta & \epsilon_{k+Q_{CDW}} \end{bmatrix} (3)$$

The eigenvalues of this matrix yield a new electronic dispersion, whose spectral weight $|u_k|^2$ is translated by $\pm\mathbf{Q}_{CDW}$ (shadow bands). This leads to the opening of a gap with amplitude of 2Δ around the crossing of main $|k\rangle$ and shadow bands $|k \pm Q_{CDW}\rangle$.

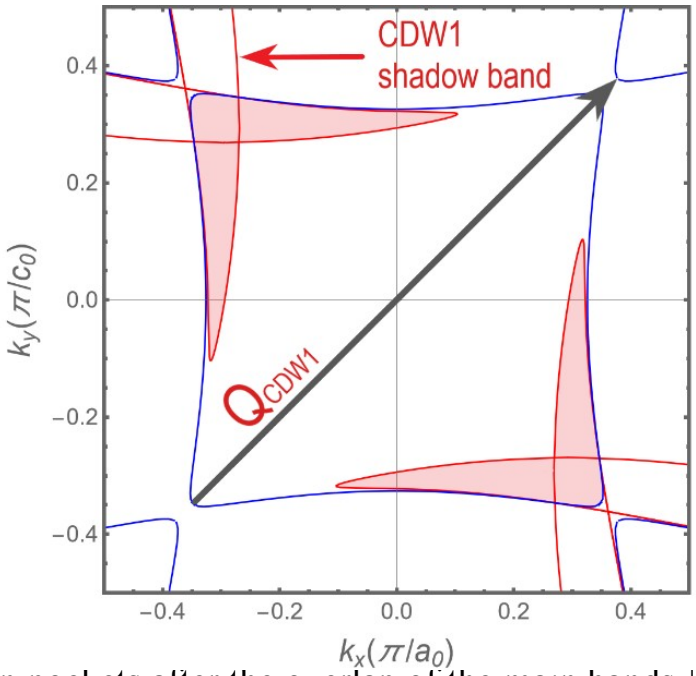

Fig. S2. Electron pockets after the overlap of the main bands $|k\rangle$ and shadow bands $|k \pm Q_{CDW1}\rangle$. Due to imperfect nesting by the CDW_1 vector, the band overlap between

the states $|k\rangle$ and $|k \pm Q_{CDW1}\rangle$ and hence the position of the gap relative to E_F shifts with momentum, which results in residual metallic pockets on the FS, marked with red color. Here, we emphasize the residual pockets inside the square part (blue square) of FS resulting from the interaction between p_x and p_y. The coupling parameter $(\Delta_1 = 0.275/2eV)$ and CDW_1 vector of $HoTe_3$ can be extracted from [3].

Experimentally, the CDW_1 gap is well seen in [4], where the part near the Fermi level is emphasized. As we can see in [4, 5], with decreasing k_y the nesting gradually weakens and residual metallic pockets appear on the FS, especially near their crossings, and therefore the system remains conducting in the CDW phase. Theoretically, the residual electron pockets (marked with red color) are shown in Fig. S2.

The first transition temperature T_{CDW1} ranges from a low temperature of 244K for $TmTe_3$, the compound with the smallest lattice parameter in the RTe_3 series, and increases monotonically with increasing lattice parameter. In contrast, measurements for the smaller lattice parameter compounds R = Dy - Tm reveal a second CDW_2 feature at a lower temperature T_{CDW2} (T_{CDW2} is largest for the heaviest member of the series) [6]. Preliminary ARPES results for $ErTe_3$ confirm this picture, revealing additional gaps forming on sections of the FS close to the tips of the diamond sections of the FS pointing in a^* direction [7]. The corresponding jump in the resistivity at T_{CDW2}, related to the amount of FS gapped at the transition, is largest for the compound with the largest value of T_{CDW2} (smallest value of T_{CDW1}) [6] and smallest area of initial FS gapped at T_{CDW1}.

The effect of the perpendicular CDW_2 is approximated using the tight biding model and illustrated in Fig. S3. The crossing regions between the coupled bands CDW_1 and CDW_2 are marked with green (blue) color. The gaps due to both CDWs are denoted with dark rectangles. As it can be noticed, the spectral weight within the nested FS regions connected by the CDW vector $\mathbf{Q}_{CDW2}$ vanishes. This results in an amount of FS gapped at the transition T_{CDW2} and hence in a reduction of the electron pockets as is shown in Fig. S3.

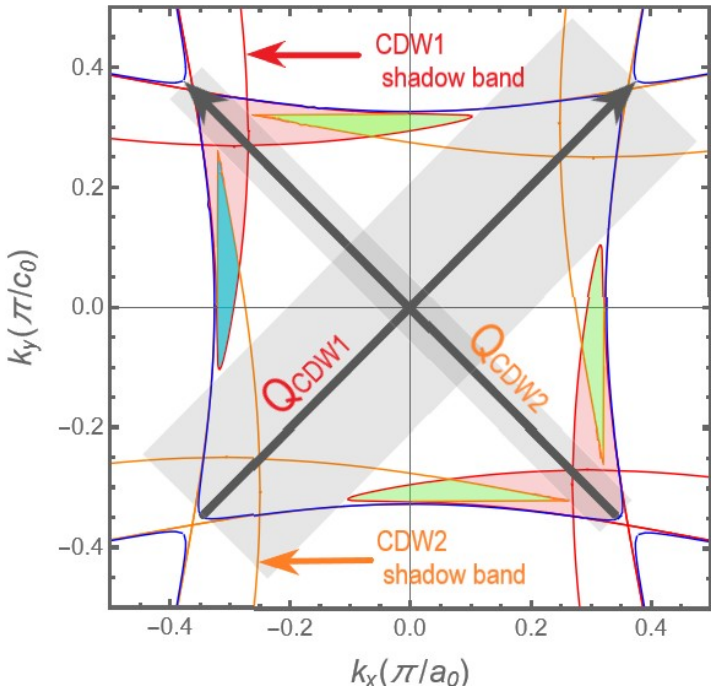

Fig. S3. Same as Fig. S2 but including the CDW_2 bands. The coupling parameter $(\Delta_2 = 0.142/2eV)$ and CDW_2 vector of $HoTe_3$ can be extracted from [3]. The crossing regions marked with green (blue) color denote the electron pockets after the overlap of the CDW bands. Monte Carlo Method will be used to estimate the area of the blue colored region.

ARPES measurements for $ErTe_3$ at $T < T_{CDW2}$ show that the spectral weight is more intense at the crossing regions between the coupled bands CDW_1 and CDW_2 [7], which will be better seen in Supplementary Note 2.

Experimentally, the electron pockets resulting from the overlap of the main bands $|k\rangle$ and shadow bands $|k \pm Q_{CDW2}\rangle$ are not visible due to the large CDW_1 gap. This is well seen in Fig. S3.

Supplementary Note 2

Electron pocket area estimation by Monte Carlo Method

Since the positions of the pockets were determined by the spectral weight in ARPES [7], we select the crossing region marked with blue color in Fig. S3 and

determine its area by Monte Carlo Method (MC), as is shown in Fig S4. The calculated Area is A_{MC} = 0.67% of the Brillouin zone (BZ).

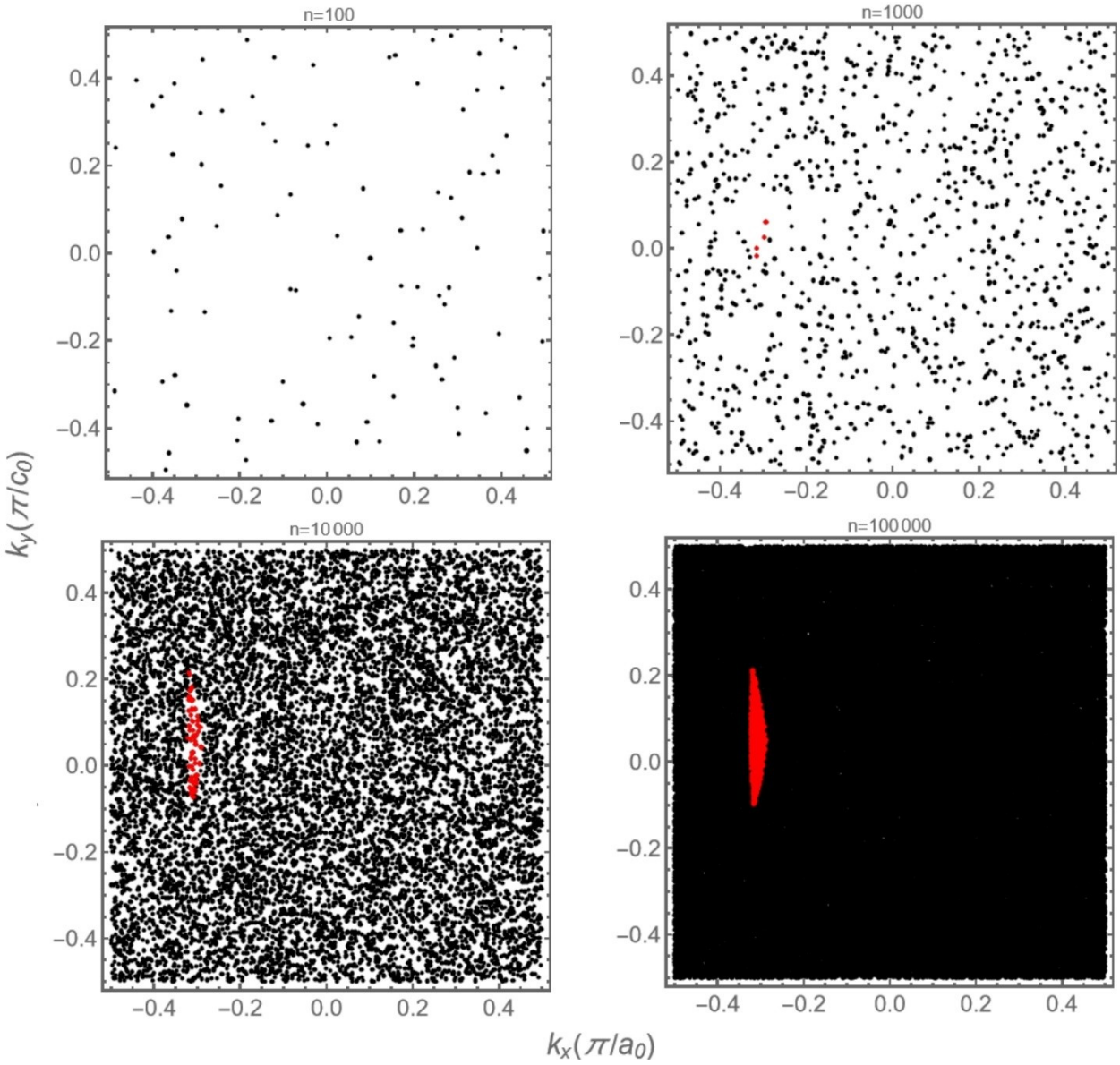

Fig. S4. MC area calculation of the region marked with blue color in Fig. S4. ***n*** is the total number of points inside the BZ.

Electron pocket area estimation from ARPES

The area estimated by MC in Fig. S4 helps us to estimate the electron pocket areas previously observed in ARPES [7] (see Fig. S5). In this case, the position of the observed pockets is fixed by mapping their intensity in the spectral weight, and then we proceed to determine the number of covered pixels as well as the coverage of the

colors. This method can give a good approximation of the area of the pockets since the area of the BZ is already known and covered with $\boldsymbol{n}$ = 100000 black points (see Fig. S4). This gives the following areas for the mapped regions **1** and **2**: $\boldsymbol{A}_{\mathbf{AR1}}$ = 0.64% and $\boldsymbol{A}_{\mathbf{AR2}}$= 0.55%, respectively.

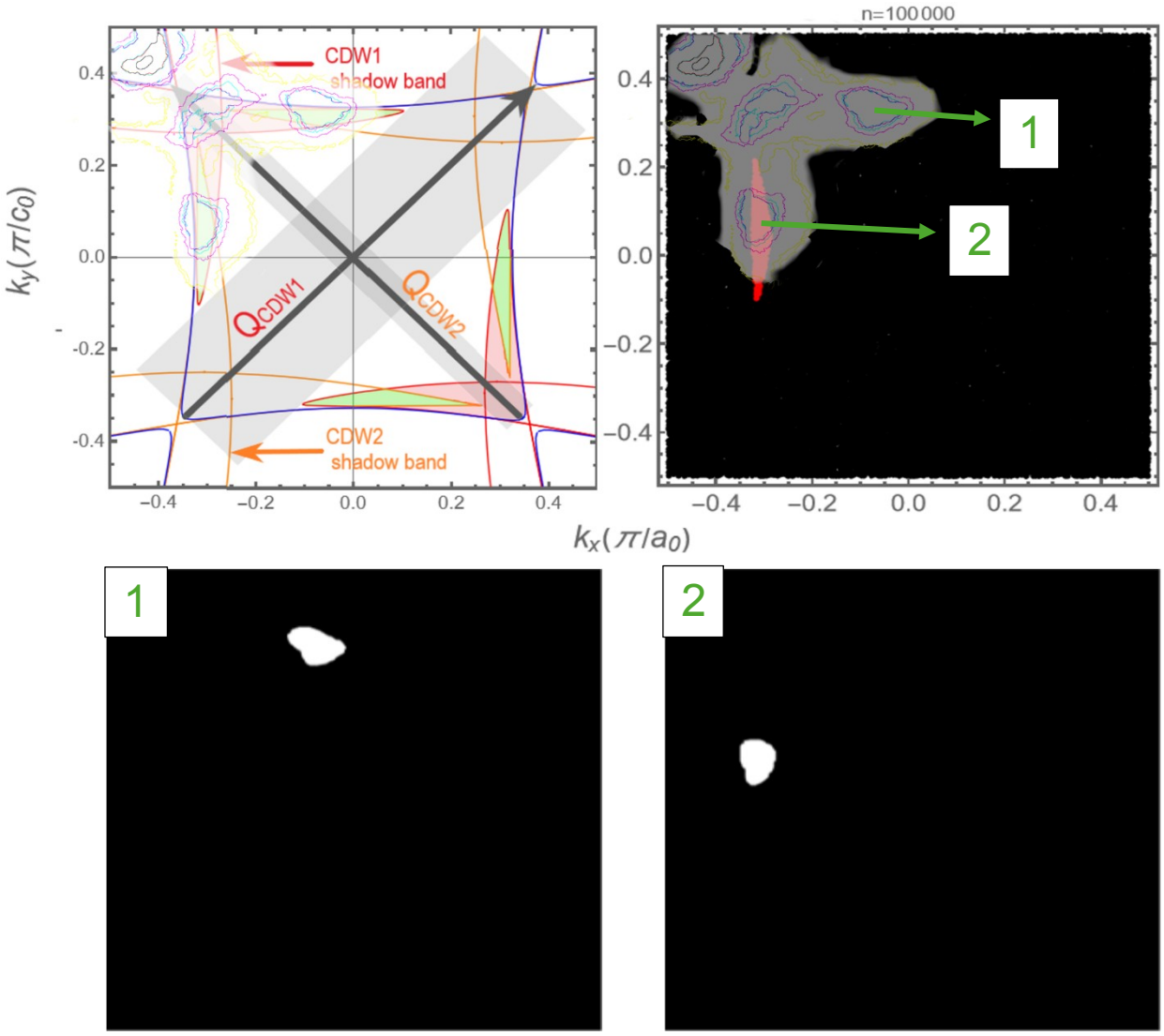

Fig. S5. Area determination of electron pockets observed in ARPES [7]. The spectral weight in $ErTe_3$ at $T < T_{CDW2}$ is fixed in the calculated bands and the location of the high-intensity regions is mapped for convenience.

As we can see from ARPES [7], the pockets shapes are not symmetrical, which is better observed in the mapped spectral weight from Fig. S5. This leads to different

pocket areas in regions **1** and **2**. Otherwise, according to TBM, the pockets should have the same area after coupling. Hence, in addition to the inaccuracy of ARPES measurements, asymmetrical shapes of the pockets make it difficult to determine the areas.

Supplementary Note 3

Frequency determination

Quantum oscillations is a direct measure of the FS area via the Onsager relation:

$$F = \left(\frac{\phi_0}{2\pi^2} \right) A_H(4)$$

where $\phi_0 = hc/2e = 2.07 \times 10^{-15}$ Tm^2 is the flux quantum, and A_H is the cross-sectional area of the FS normal to the applied field [8]. This results in the following frequencies:

Area		Frequency
$A_{\mathbf{MC}} = 0.67\%$	⟶	151 T
$A_{\mathbf{AR1}} = 0.64\%$	⟶	144 T
$A_{\mathbf{AR2}} = 0.55\%$	⟶	124 T

A frequency of 124 T implies a Fermi surface pocket that encloses a k-space area of A_H = 0.55 % of the Brillouin zone.

The approximation can be improved by considering the region of intersection between $\mathbf{A_{MC}}$ and $\mathbf{A_{AR2}}$ ($A_{MC \cap AR2} = 0.3\%$) which gives a frequency of F = 67 T. Although the Onsager relation predicts lower areas for peaks observed in the quantum oscillation frequency spectrum in Fig. 4 of the main manuscript, the approximation given by us is very good despite the inaccuracy of the ARPES measurements.

It should be mentioned that the CDW gaps ($2\Delta_1=175$ meV and $2\Delta_2=50$ meV [7]) for $ErTe_3$ are smaller than the gaps for $HoTe_3$, and that the spectral weight distributed on the translated parts of the band structure strongly depends on the CDW vectors. This results in a larger margin of error in our calculation after the reconstruction of the FS in the TB model.

1. P. A. Vorobyev, P. D. Grigoriev, K. K. Kesharpu, and V. V. Khovaylo, *The Evolution of Electron Dispersion in the Series of Rare-Earth Tritelluride Compounds Obtained from Their Charge-Density-Wave Properties and Susceptibility Calculations*, Materials **12**, 2264 (2019). https://doi.org/10.3390/ma12142264.

2. V. Brouet W. L. Yang, X. J. Zhou, Z. Hussain, R. G. Moore, R. He, D. H. Lu, Z. X. Shen, J. Laverock, S. B. Dugdale, N. Ru, and I. R. Fisher, *Angle-Resolved Photoemission Study of the Evolution of Band Structure and Charge Density Wave Properties in RTe_3 (R=Y, La, Ce, Sm, Gd)*, Physical Review B **77**, 235104 (2008). https://doi.org/10.1103/physrevb.77.235104.

3. R. Lou, Y. Cai, Zh. Liu, T. Qian, L. Zhao, Y. Li, K. Liu, Zh. Han, D. Zhang, J. He, G. Chen, H. Ding, and Sh. Wang, *Interplay between Multiple Charge-Density Waves and the Relationship with Superconductivity in Pd_xHoTe_3*, Physical Review. B **93**, 115133 (2016). https://doi.org/10.1103/physrevb.93.115133.

4. V. Brouet, W. L. Yang, X. J. Zhou, Z. Hussain, N. Ru, K. Y. Shin, I. R. Fisher, and Z. X. Shen, *Fermi Surface Reconstruction in the CDW State of $CeTe_3$ Observed by Photoemission*, Physical Review Letters **93**, 126405 (2004). https://doi.org/10.1103/physrevlett.93.126405.

5. L. Rettig, R. Cortés, J. -h. Chu, I. R. Fisher, F. Schmitt, R. G. Moore, Z. -x. Shen, P. S. Kirchmann, M. Wolf, and U. Bovensiepen, *Persistent Order Due to Transiently Enhanced Nesting in an Electronically Excited Charge Density Wave*, Nature Communications **7**, 10459 (2016) https://doi.org/10.1038/ncomms10459.

6. N. Ru, C. L. Condron, G. Y. Margulis, K. Y. Shin, J. Laverock, S. B. Dugdale, M. F. Toney, and I. R. Fisher, *Effect of Chemical Pressure on the Charge*

Density Wave Transition in Rare-Earth tritellurides RTe_3, Physical Review B **77**, 035114 (2008). https://doi.org/10.1103/physrevb.77.035114.

7. R. G. Moore, V. Brouet, R. He, D. H. Lu, N. Ru, J. -h. Chu, I. R. Fisher, and Z. -x. Shen, *Fermi Surface Evolution across Multiple Charge Density Wave Transitions in $ErTe_3$*, Physical Review B **81**, 073102 (2010). https://doi.org/10.1103/physrevb.81.073102.
8. J. M. Ziman, *Principles of the Theory of Solids*, 2nd ed. Cambridge University Press, (1972). https://doi.org/10.1017/cbo9781139644075.